

Numerical Methods to Simulate Turbulent Dispersed Flows in Complex Geometries

E. Bayraktar*, R. Münster, O. Mierka and S. Turek

Institute of Applied Mathematics (LS III), TU Dortmund
Vogelpothsweg 87, D-44227, Dortmund, Germany.

E-mail: ebayrakt@math.uni-dortmund.de

Abstract

Population Balance is a prominent ingredient of modeling transport phenomena. Population Balance Equations (PBEs) are coupled to Computational Fluid Dynamics (CFD) to simulate turbulent dispersed flows. One of the arising challenges is to obtain an appropriate discretization technique for the internal coordinate of PBEs, so the resulting equations can lead to acceptable solutions with affordable computational costs in reasonable time scales. On the other hand, geometries in the industrial problems can be very complex such that pre-processing steps require great effort and time, especially for pure hexahedral meshes. Nevertheless, instead of conventional meshing tools, a different approach based on the concept of “fictitious domains”, Fictitious Boundary Method (FBM), can be employed to mesh complex, moving and/or deforming geometries. In this study, we present efficient implementation strategies and numerical methods to couple PBEs to CFD and numerical simulation techniques using a finite element approach in combination with FBM. The presented methods are validated with a study of Sulzer static mixer, SMVTM [1], and simulations of rigid particulate flows [2], which were achieved in the FEATFLOW environment.

Keywords: Population Balance Equations; Fictitious Boundary Method; Static mixer; Twin-screw extruders

1. Introduction

The chemical engineering community began the first efforts of association with the concepts of the population balance in the 1960s, while population balances may be regarded either as an old subject that has its origin in the Boltzmann equation more than a century ago. On the other hand, population balances are certainly considered as a new research field in light of the variety of applications in which engineers have recently put population balances to use. There is an intensive ongoing research in this field by researchers of many different backgrounds. Applications cover a wide range of dispersed systems, such as crystallization systems (solid-liquid), aerobic fermentation (gas-liquid) and food processes (liquid-liquid), and in this study will be focused on liquid-liquid dispersed systems in complex geometries.

In practical applications, a single bubble/droplet size model, as reported by numerous researchers [3, 4], cannot properly describe the interfacial interactions between the phases, and analytical solutions of the PBE are available just for very few and specific cases. Hence, the use of appropriate numerical techniques is unavoidable in order to

deal with practical problems. There are several numerical methods satisfying the necessary requirements with respect to robustness and realizability: the quadrature method of moments [5, 6], the direct quadrature method of moments (DQMM) [7], parallel parent and daughter classes (PPDC) [8] and the method of classes (MC) [9, 10]. Among these available techniques, the last one is chosen to discretize the internal coordinate in this study.

Population Balance Equations (PBEs) of liquid-liquid dispersed systems involve breakage and coalescence kernel functions which are the mathematical formulation of all the physics in breakup and coalescence phenomena. There are many studies available about modeling of coalescence and modeling of breakage and a detailed review of these studies was presented by Jakobsen et al. [12]. While it is possible to gather coalescence kernels into a unified framework, the breakage kernels show distinct behaviors and their formulations can exhibit remarkable differences. The breakage kernels can be classified as statistical, theoretical and phenomenological. For our purposes, we had chosen a theoretical kernel which is derived from one of the most well known theoretical breakage kernel by Luo and Svendsen [13], is valid for a wide range of operating conditions and has a good convergence behavior for the solution of PBE. Most of the present models for coalescence kernels were derived analogously to kinetic theory of gases [14, 15, 16, 17]. In kinetic theory of gases, collisions between molecules are considered while in the process of coalescence, bubble (droplet)–bubble (droplet) and bubble/droplet–eddy collisions count. The coalescence kernel adopted in this work is the one proposed by Lehr *et al.* [18] which is implemented according to the technique developed by Buwa and Ranade [19]. Both breakage and coalescence kernels involve terms which are hydrodynamic variables and are obtained from the result of CFD calculations. (For further discussion of breakage kernels and coalescence kernels adopted in this study the reader is referred to Bayraktar et al. [1].)

In order to solve the PBEs one should be able to firstly resolve the flow field in the computational domain. Therefore, PBEs should be coupled to the governing equations of turbulent fluid dynamics. This inevitable coupling is one of our main focus and issued in detail by Bayraktar et al. [1]. CFD simulation of dispersed phase systems has been a topic of research for the last several decades and many different methods were developed. Numerical simulations which assume the flow to be laminar are not able to produce mesh independent results. The finer the grid, the more vortices are resolved. That is more typical for turbulent flows. Turbulence models which are applicable to produce results with an acceptable accuracy and reasonable computational cost in general originate from the family of two-equation eddy viscosity models. The most preferred model in this sense is related to the standard or modified k - ε two equation turbulence model which have both been implemented to our in-house code, FeatFlow [4].

The availability of experimental and numerical results in the literature for perfectly stirred tank reactors made it possible to validate and verify our implementation in 0D. Nevertheless, there were no comprehensive experimental and numerical data in the literature to verify the 3D implementation. Therefore, after our implementation is validated in [1], we did several experiments which cover a wide range of operation conditions with SMVTM static mixers in Sulzer Chem Tech Laboratories (Winterthur, Switzerland) to be able to verify our implementation for different operating condition.

The computational domain which was used in the simulation of dispersed flow through the SMVTM static mixers was very complex as it is the case in most of the industrial problems. In these cases, pre-processing may require quite a bit of hand work and can be very time consuming if it is possible at all. An alternative approach is based on the concept of 'fictitious domains'. The idea of this Eulerian method is to simulate the presence of an additional domain, the 'fictitious domain', inside the computational domain. This in turn implies the existence of a boundary between these domains which is realized by adding appropriate terms to the mathematical model. The idea was first published by Glowinski, Joseph, Patankar and coauthors [20, 21], who proposed an approach based on a distributed Lagrange multiplier (DLM)/fictitious domain method for the direct numerical simulation of large number of rigid particles in fluids. Our group proposed another multigrid fictitious boundary method (FBM) based on the boundary conditions applied at the interface between the obstacle and the fluid which can be considered as an additional constraint to the governing Navier-Stokes equations [22, 23, 24]. An advantage of these fictitious domain methods over the generalized standard Galerkin finite element method is that the fictitious domain methods allow a fixed grid to be used in case of moving geometries [2]. The capabilities of this method is presented with a case study, a twin-screw extruders.

The paper is organized as follows: In Section 2 the governing equations and their closures are presented. The following section issues the employed numerical techniques. The experimental set up and methodology is given in Section 4. The experimental and numerical results are compared in Section 5. In Section 6, a case study involving twin-screw extruders is shown which is followed by our conclusions and outlook.

2. Mathematical model

The population balance equation for liquid-liquid/gas dispersions is a transport equation of the number density probability function, f , of bubbles (drops). By definition, f needs to be related to an internal coordinate, what in most of the cases is the volume of bubbles (drops), v . Therefore, the number density, N , and void fraction, α , of bubbles having a volume between v_a and v_b are:

$$N_{ab} = \int_{v_a}^{v_b} f dv, \quad \alpha_{ab} = \int_{v_a}^{v_b} f v dv. \quad (1)$$

The considered transport phenomena account for convection in the spatial space (governed by the flow field \mathbf{u}_g), while the bubble breakage and coalescence move the bubbles in the internal coordinate. Thus, the resulting transport equation is the following

$$\frac{\partial f}{\partial t} + \mathbf{u}_g \cdot \nabla f = B^+ + B^- + C^+ + C^-. \quad (2)$$

Clearly, in case of modeling turbulent flows according to (temporal) averaging, the concepts (2) has to be extended by the arising pseudo diffusion terms in analogy to the approach of the Reynolds stress tensor

$$\nabla \cdot \overline{u'f'} = -\nabla \cdot \left(\frac{\nu_T}{\sigma_T} \nabla \bar{f} \right), \quad (3)$$

where σ_T is the so-called turbulent Schmidt number. In (2) the superscripts ”+” and ”-” stand for sources and sinks and the terms B and C on the right hand side represent the rate of change of the number density probability function, $(\frac{df}{dt})$, due to bubble breakup and coalescence, respectively. These terms are the closures of our governing equations and they are adopted from the study of Lehr et al. [18] after a detailed study which focused on the numerical behaviors and the valid range of operating conditions [1]. With introducing the complete formulation of source and sink terms, our governing equation turns out to be a strongly non-linear unsteady integro-differential equation whose solution is numerically very challenging and closed with the chosen breakage and coalescence kernels:

$$\begin{aligned} \frac{\partial f}{\partial t} + \mathbf{u}_g \cdot \nabla f = & \int_v^\infty r^B(v, \tilde{v}) f(\tilde{v}) d\tilde{v} - \frac{f(v)}{v} \int_0^v \tilde{v} r^B(\tilde{v}, v) d\tilde{v} \\ & + \frac{1}{2} \int_0^v r^C(\tilde{v}, v - \tilde{v}) f(\tilde{v}) f(v - \tilde{v}) d\tilde{v} - f(v) \int_0^\infty r^C(\tilde{v}, v) f(\tilde{v}) d\tilde{v} \end{aligned} \quad (4)$$

The fluid dynamic terms which appear in (4) exhibit a strong coupling between turbulent fluid dynamics and PBEs. The turbulent model and the one-way coupling approach of CFD-PBE which are employed in our implementation are explained in detail in our preceding study [1].

3. Numerical methods

Solutions of PBE involve the solution of integro-differential equations. In 0D, that means ideally stirred tank reactors, when the equation is discretized in time, one is left with the evaluation of integral equations. However, in 3D, even after time discretization, the equation is still an integro-differential equation which has to be numerically treated very carefully. The employed numerical tools have to be chosen in a way that the required computational time and computational cost is minimum while the numerical scheme is robust and the results are accurate.

The main numerical challenges in the solution of coupled CFD-PBE problems are the same with the one in turbulent flow problems and additionally, difficulties involved in the solution of PBE. Since the equations are coupled and eventually (4) is needed to solve, the challenge of developing a positivity preserving bounded numerical scheme arises in order to solve a transport problem where the transported quantity is non-diffusive or with a very low diffusivity which can be less than even numerical diffusivity added to the solution due to the spatial discretization and/or stabilization scheme of the convective term. These are difficulties considering the accuracy, on the other hand the chosen numerical ingredients have to match to establish a robust and efficient scheme. For example, to have upwind stabilization scheme with a MC discretization of PBE can be working fine; however, it is a question if it would work with MoM.

The employed numerical techniques to establish a positivity preserving bounded scheme and to have a robust turbulence model with the appropriate time discretization scheme are given in [1, 26, 25]; here, we discuss the numerical techniques to discretize the PBE and how to mesh complex boundaries with pure hexahedral cells.

3.1. Discretization of the internal coordinate

As analytical solutions of PBEs are available in very few cases, numerical techniques are essential in most practical applications. Such techniques are sought to be accurate with a relatively low computational cost. There are several available numerical methods satisfying the accuracy requirement. Among them are the Monte Carlo method [27], the methods of classes (MC) [9, 10], the quadrature method of moments (QMOM) [5, 6], the direct quadrature method of moments (DQMOM) [7], parallel parent and daughter classes (PPDC) [8] and the standard method of moments (SMM) in some simple cases. These techniques can be classified as class based and moment based methods. First we will discuss these techniques in 0D and 3D then the discrete reformulation of (2) will be presented in terms of void fractions.

In 0D, when the interest is on some statistical values of droplet population as, d_{32} , d_{30} , d_{23} , moment based methods are clearly superior to class based methods. The conservation of higher order of moments and requirement of less arithmetic operations for the same problem are the advantages of moment based methods. However, if one needs to know the droplet size distribution (DSD), it has to be reconstructed from the available appropriate techniques and most of the time it is a question: does the reconstruction techniques lead us to the physical distribution. The available reconstruction techniques and their detailed discussion are given by John et al. [28].

In 3D, additional to the reconstruction problem of DSD, the transport of moments has to be calculated very accurately. The product difference algorithm [29] which is used in PPDC or QMOM is ill conditioned and small perturbations on the values of moments can deteriorate the solution and the whole scheme fails due to unphysical values, negative droplet sizes or negative void fractions. And in complex geometries or when flow field changes rapidly (existence of steep gradients), the accurate transport of moments turns out to be very cumbersome if it is possible at all. For an acceptable accuracy, one has to reduce the time step size and employ computationally costly numerical techniques, algebraic flux correction schemes [26]. Otherwise, added numerical diffusion may perturb the actual values of moments and the implementation fails in product difference algorithms. Even though all the appropriate numerical ingredients are gathered together, nothing guarantees that the implementation with moment based methods will be robust. Therefore, our choice of discretization technique for the internal coordinate was mostly influenced by the robustness criterion which was clearly in favor of class based methods.

The discretization of the PBEs (4) with MC is carried out by adopting the fixed pivot approach:

$$\begin{aligned} \frac{\partial f_i}{\partial t} + \mathbf{u}_g \cdot \nabla f_i - \nabla \cdot \left(\frac{\nu_T}{\sigma_T} \nabla f_i \right) &= \sum_{j=i}^n r_{i,j}^B f_j \Delta v_j - \frac{f_i}{v_i} \sum_{j=1}^i v_j r_{j,i}^B \Delta v_j \\ &+ \frac{1}{2} \sum_{j=1}^i r_{j,k}^C f_j f_k \Delta v_j - f_i \sum_{j=1}^n r_{j,i}^C f_j \Delta v_j \quad \text{for } i = 1, 2, \dots, n \end{aligned} \quad (5)$$

The fixed pivot volume of the classes is initialized by specifying the bubble volume of

the smallest class and the discretization factor. The choice of fixed bubble pivot volumes and fixed class widths offers the advantage of expressing the discretized transport equation (5) in terms of class holdups α_i instead of the number probability density, $f_i = \frac{\alpha_i}{v_i \Delta v_i}$ (see (1)). Doing so enforces mass conservation, however the bubble number density may not be conservative. Regarding the arising inconsistency we subscribe to the argument of Buwa and Ranade [19], who reported that the difference in the predicted values of interfacial area and Sauter mean bubble diameter obtained with only mass conservation and obtained with mass and bubble number conservation was less than 1%. Then the discretized transport equation of the i -th class' void fraction reads:

$$\begin{aligned} \frac{\partial \alpha_i}{\partial t} + \mathbf{u}_g \cdot \nabla \alpha_i - \nabla \cdot \left(\frac{\nu_T}{\sigma_T} \nabla \alpha_i \right) &= \sum_{j=i}^n r_{i,j}^B \frac{\alpha_j}{v_j} v_i \Delta v_i - \frac{\alpha_i}{v_i} \sum_{j=1}^i v_j r_{j,i}^B \Delta v_j \\ &+ \frac{1}{2} \sum_{j=1}^i r_{j,k}^C \frac{\alpha_j}{v_j} \frac{\alpha_k}{v_k \Delta v_K} - \alpha_i \sum_{j=1}^n r_{j,i}^C \frac{\alpha_j}{v_j} \quad \text{for } i = 1, 2, \dots, n \end{aligned} \quad (6)$$

However, when (6) is discretized in time and space within a finite element approach, the discrete system of equations to be solved is slightly different. To be able to have a positivity preserving scheme the sinks term are treated implicitly on the left hand side with the unknowns and source terms are treated explicitly on the right hand side with the initial guess/solution. For the details of complete implementation the reader is referred to [1].

3.2. Fictitious boundary method

The multigrid FEM fictitious boundary method (FBM) [30, 31, 32] is based on a multigrid FEM background grid which covers the whole computational domain and can be chosen independent of the geometry of interest. It starts with a coarse mesh which may already contain many of the geometrical details, and it employs a fictitious boundary indicator (see [30]) which sufficiently describes all fine-scale features. Then, all fine-scale features are treated as boundaries such that the corresponding components in all matrices and vectors are modified according to the assigned boundary condition. The considerable advantage of the multigrid FBM is that the total mixture domain does not have to change in time, and can be meshed only once.

Traditionally geometries used in this approach are restricted to analytically described ones. This restriction limits this powerful tool to be used for few cases; however, it is possible to use FBM for general geometries with our approach. This is accomplished by representing the geometry as a surface triangulation, which is basically a piecewise linear approximation of the geometry's surface. This type of geometry is widely used in CAD, CAGD and computer graphics in general. In preliminary work our group developed efficient techniques for solving the geometric problems and showed that the geometry discretization error has no significant influence on the error of the numerical solution because the error due to the spatial discretization of the domain is significantly larger

than the error of the geometry discretization [34, 33]. The details of our implementation are given within a framework of particulate flow [2].

4. Experimental studies

The experiments are designed to simulate the effect of void fraction and turbulent dissipation rate on the resulting size distribution of the dispersed phase. In experimental set-up, Figure 2, Sulzer static mixers SMVTM (DN25) was used to exploit the mixing quality for different flow rates. In all experiments, water and oil were the primary and the secondary phases, respectively, with the following physical properties,

- density of water, $\rho_w = 1000 \text{ kg m}^{-3}$;
- density of oil, $\rho_o = 847 \text{ kg m}^{-3}$;
- viscosity of water, $\mu_w = 1 \text{ mPa s}$;
- viscosity of oil, $\mu_o = 32 \text{ mPa s}$;
- interfacial tension, $\sigma_{wo} = 0.043 \text{ N m}^{-1}$.

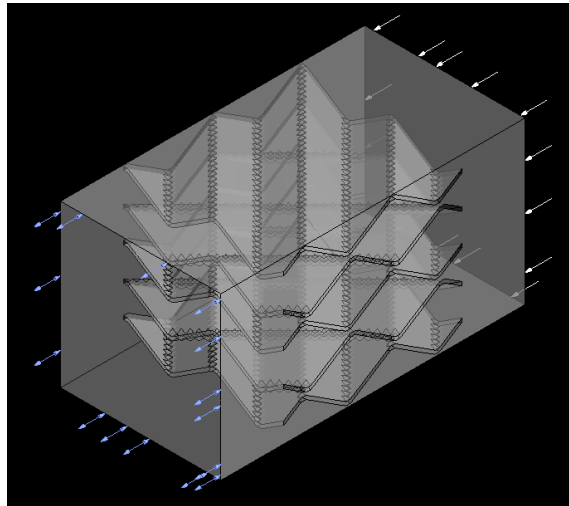


Figure 1: The geometry of case 1SMV.

The test rig, Figure 2, was designed modularly allowing to alter the position of the measurement section, Liquid-Liquid In-Line Sizing Apparatus (LLISA). LLISA owes enhanced magnification abilities to microscope objectives. In this measurement technique, the underlying assumption is: time integrated count of bubbles/droplets which are captured in the photographed volume represent time averaged size distributions of population in the cross section where LLISA is placed. Thus, the gap between the two windows of LLISA (at the bottom of the hollow threads where the flash and camera are placed) should always be more than a certain width in order not to have a filtering effect for the large droplets.

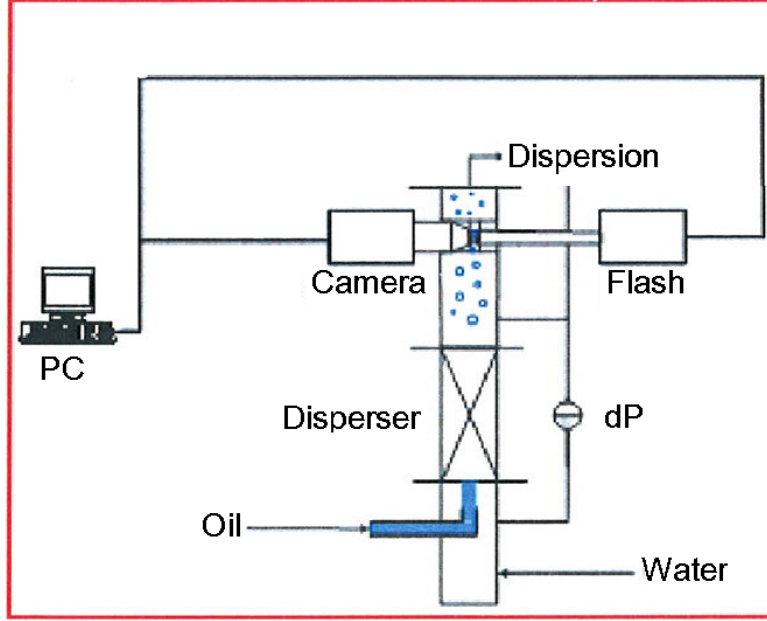


Figure 2: Experimental set-up in Sulzer Chem Tech laboratories.

The camera and the flash of LLISA are triggered simultaneously and the taken pictures are sent to a computer so to be saved in disc drive of the computer. Then, the pictures are processed manually to evaluate the droplet size by "Bubble Count" software which is provided by Sulzer Chem Tech.

The measured radii are in the unit of pixel and they have to be converted to actual sizes with a conversion factor. The required factor was obtained by taking several pictures of calibration slide. Then, the mean value and standard deviation of these measurements were calculated in order to determine the conversion factor and the accuracy of our measurements. The conversion factor and the standard deviation were found to be $2.5 \times 10^{-6} \text{ m px}^{-1}$ and 2 px which is equal to $5 \times 10^{-6} \text{ m}$. After obtaining the conversion factor, the mean diameter and standard deviation of the mean is calculated for each case. Moreover, we suggest a post-processing without adding any more assumptions to the problem. The measured droplets (v_m) are assigned to certain classes (with v_i^{min} and v_i^{max} being lower and upper limit of the i 'th class, respectively) as it is done in numerical simulations,

$$\text{if } v_m \in [v_i^{min}, v_i^{max}), \quad v_m = n_i m v_i \quad (7)$$

where n_{im} is the weight factor of droplet v_m for i 'th class. Then, the volume of the measured droplets added to their corresponding classes. Finally, we obtain a volume distribution for an arbitrary volume of the secondary phase. However, we know that this arbitrary volume should actually be the integrated volume of the secondary phase in a certain control volume in time, because all the measurement set-up was developed based on this assumption. This knowledge leads us to calculate a discrete probability distribution (DPD) of the holdup (or volume, DPD is the same for both). Dividing the volume assigned to each class by total volume leads to the following definition of DPD.

$$Pr_i = \frac{v_i^T}{v^T}, \quad \sum v_i Pr(X = v_i) = 1 \quad (8)$$

Then, the holdup distribution of i 'th class is calculated as:

$$\alpha_i = Pr_i \alpha \quad (9)$$

As a consequence, the measured droplet sizes are evaluated in a way which allows to compare the hold up distribution obtained in numerical simulations and experiments.

5. Results and discussion

In this section, we present the numerical and experimental results. First, the results of our numerical studies on the simulation of oil in water dispersions through SMVTMstatic mixer are given and compared with experimental results which is followed by our discussion. Later, a case study of twin-screw extruders is presented in order to give an insight to the capability of our FEM-FBM implementation.

5.1. SMVTM static mixer

We designed the experiments and corresponding numerical simulation in order to show the effect of flow field and the effect of void fraction of the secondary phase on the final DSD, for a certain holdup value we studied different flow rates and vice versa. The studied holdup values are 5%, 10%, 15% of the secondary phase and values of inlet velocity are 1 ms⁻¹, 1.25 ms⁻¹ and 1.5 ms⁻¹. The physical properties of the fluids are given in Section 4 where the experimental setup is described.

We adopted a stationary one-way coupled CFD-PBE approach to reduce the extensive computational cost. First, a quasi-stationary flow field solution is obtained since there is no true stationary flow field solution in turbulent regime. Then, these solutions are interpolated to a coarser mesh, the grid size which is used for turbulent flow calculations is unnecessarily fine to solve PBE. The discrete internal coordinates which are used in evaluation of experimental results are the same with the ones in numerical studies in order to compare experimental results and numerical results. Nevertheless, since the internal coordinates which are used for the numerical computations are too fine for the experimental results, both results are mapped onto a coarser grid which has doubled grid size of the finer one. The following plots, Figure 3, show the experimental and numerical results.

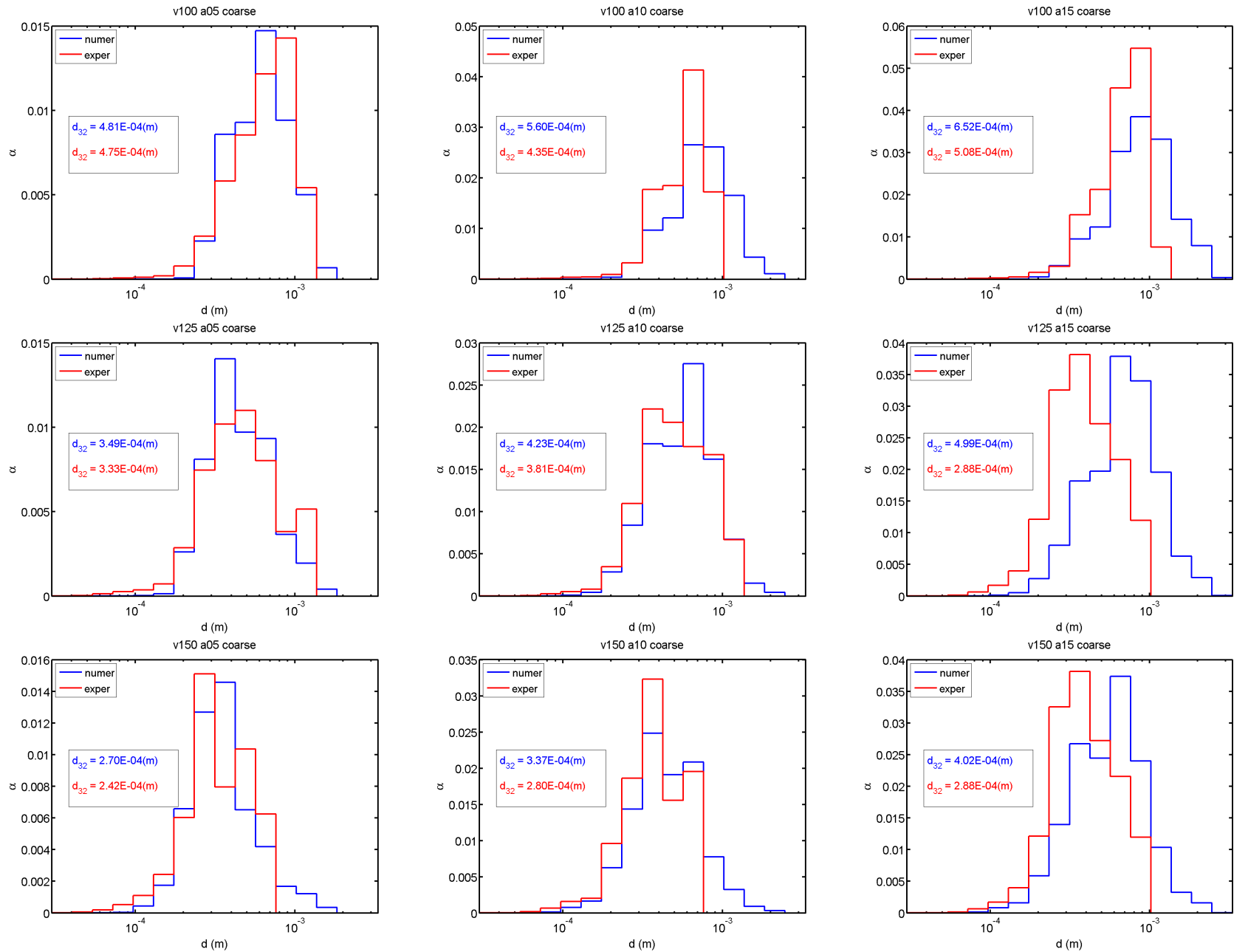


Figure 3: 1SMV; inlet velocity: 1.00, 1.25, 1.50 m s^{-1} , holdup: 0.05, 0.10, 0.15; rows: increasing holdup, columns: increasing velocity.

When the plots at the first row and the first column in Figure 3 are considered, the agreement in the results is more than being satisfactory. Nevertheless, this is an expected consequence that the discrepancies between the results would be small for lean dispersions and less turbulent flows. There are mainly two reasons. First, the models are mostly developed for lean dispersions and their prediction capabilities get worse with an increase of the secondary phase fraction. Second, the CFD results of less turbulent flows are more accurate because as the Reynolds number increase, the effect of the unresolved subgrid scales becomes more influential on the main flow. However, these are not the only reasons which can explain the differences between the results. For instance, a single phase model was used in CFD calculations so the effect of change of the holdup value on the flow field could not be simulated. Although the physical qualities of the fluids are very similar, the assumption will certainly become rougher with an increase secondary phase fraction. Moreover, the experimental results have some accuracy problem inherited in the experimental setup and these may have a significant role in the disagreement of results. First of all, the pictured droplets can be more accurately evaluated for low hold up and velocity values since the taken pictures for these cases are more clear and sharper. Additionally, the distance between the flash and camera windows of LLISA should be small to obtain clear pictures in case of high holdup and/or high flow rates, and this can result in a filtering effect for the large droplets and they are not captured in the shots. This argument is supported with our experimental and numerical results. While the largest bubble size increasing with an increase of the holdup for the same flow rate, in experimental results, this is not the case. When the experimental results in the second row (Figure 3) are compared, this consequence is visible.

5.2. Twin-screw extruder simulations

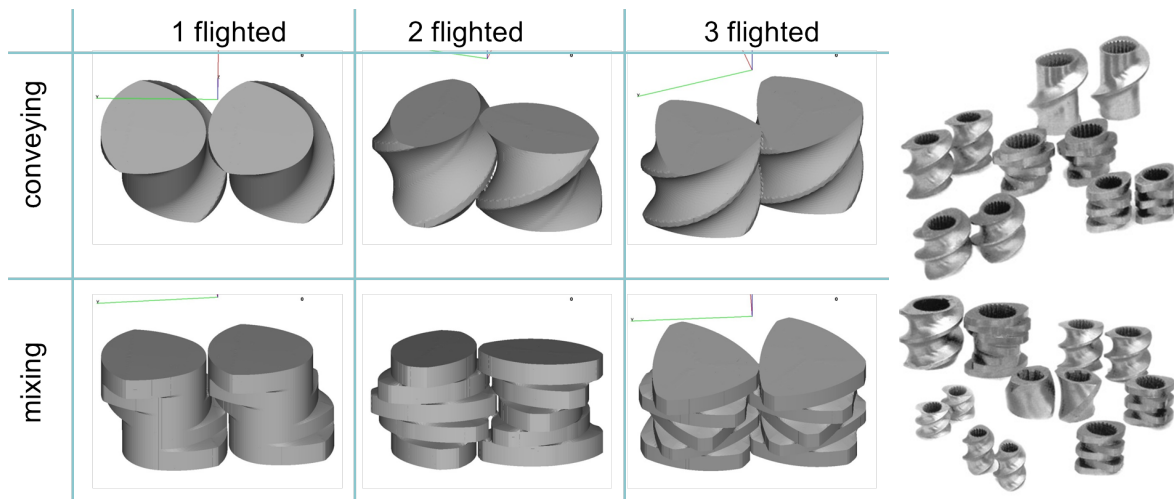


Figure 4: Left: classification of twin-screw elements. Right: real elements available on the market.

Twin-screw extruders are material processing units especially used in the industry related to plastics extrusion. In this case of application the process commonly starts with

feeding dried plastic pellets into the feed screw. The polymer resin is then heated to molten state by a combination of heating elements and shear heating from the extrusion screw. For this reason there are different sections identified during the extrusion process starting with the solids conveying section, continuing with the melting section and finishing with the melt-conveying section. From the CFD simulational point of view the last section is the most interesting where the highly viscous (and in most of the cases shear thinning) polymeric materials are already flowing (forming a continuum) and completely fill up the free space between the outer shell and the extruder elements. Simulation of the given process becomes then very challenging due to the following reasons:

- the geometry of interest is complex: it may include sharp edges and due to the rotation of the screws it changes,
- due to the small gaps (between the outer shell and mixing elements or mixing elements and mixing elements) small irregularities are present in the flow,
- the fluid exhibits non-Newtonian and temperature dependent rheological behavior,
- presence of hot spots due to local heat dissipation caused by extreme shear rates.

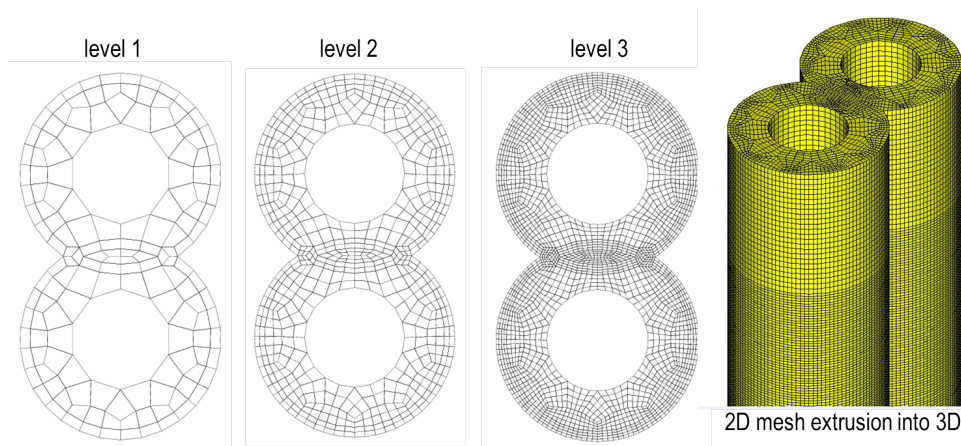


Figure 5: Employed computational meshes for the simulations of the twin-screw extruders.

While the first two points affect resolution and meshing related strategies the next two influence the model and its implementation and the resulting convergence. In this contribution we focus only on the mesh and resolution related issues and their respective treatment by the Fictitious Boundary Method (FBM). According to the given method, independently of the exact shape description (for a more consistent overview see Fig. 4, which contains a basic classification of twins-screw elements in comparison with the industrially used ones) of the modeled elements a general coarse grid is generated. The generated mesh only captures the (static) outer shell of the twin-screw extruder and includes the pre-refined regions where the highest resolution is required. Such generated meshes in 2D and their subsequent 'extrusion' into 3D are given in Fig. 5. According to the FBM an identifier field is generated at every time step with respect to all degrees of freedom (dof), which evaluates the presence of fluid or fictitious domain. Then, in

the fluid domain the Navier-Stokes equations are solved with the underlying rheological models, while in the fictitious domain rotational Dirichlet boundary conditions are to be imposed. As next a short demonstration of the FBM based approach follows on the example of polyamid extrusion in conveying two-flighted twin-screw extruder. In this case the prescribed mass flow is set to be 70 g/s and the angular rotation of the screws is set to 10 Hz. The extruded material is described with the Carreau model of the following type:

$$\mu = \frac{61.2}{(1 + 0.0005 \|\dot{\gamma}\|)^{0.3201}} [Pa s]$$

The resulting distribution of pressure and velocity for a given instance is given in Fig. 6.

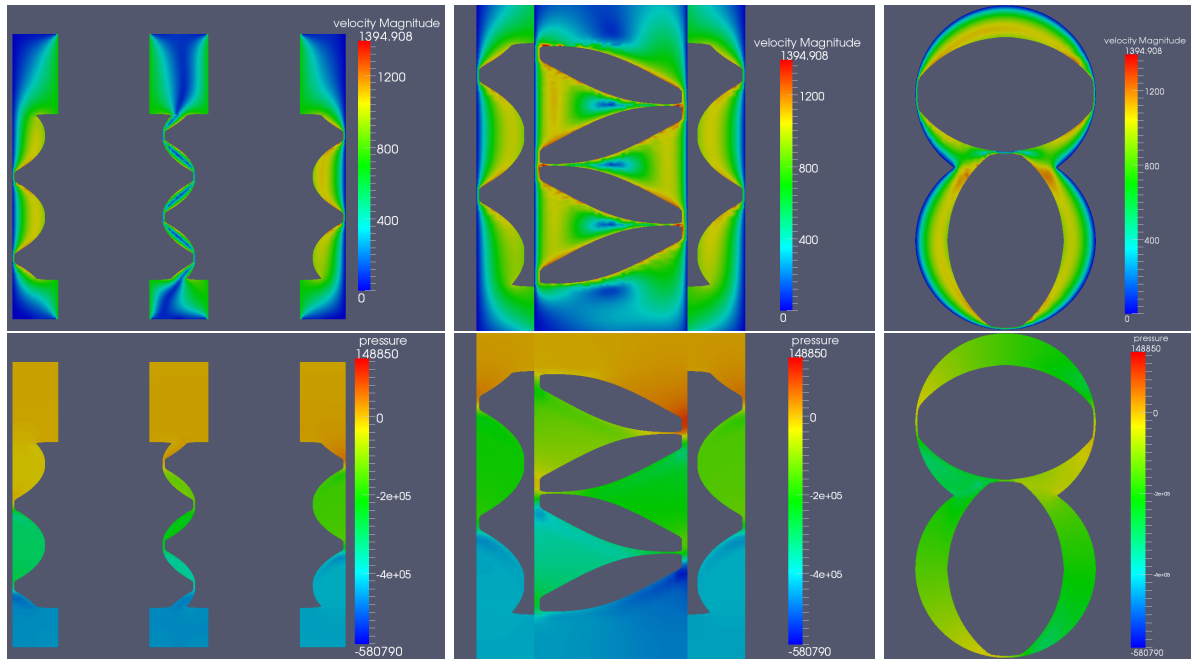


Figure 6: Resulting velocity magnitude (up) and pressure (down) distributions at X, Y and Z normal cross sections.

6. Conclusion

The dynamics of liquid-liquid flow in Sulzer static mixer SMVTM were studied using experiments as well as CFD simulations. A population balance equation was employed to predict bubble-size distributions by modeling the breakup and coalescence processes of bubbles. The experimental data is evaluated with the suggested method and the experimental and numerical results were compared. The main findings are as follows: the implemented model has good predictions for low turbulent dissipation rate and lean dispersions, for high holdup and/or high flow rates, there is a certain disagreement of the results. The reasons and possible improvements were discussed in section Results and

Discussion. Consequently, our population balance implementation is verified with this numerical and experimental study.

Numerical simulation of twin-screw extruders is studied in order to show the capabilities of FBM. The rotating complex geometry was a challenging and comprehensive test case for FBM, handling complex and moving geometries. With this case study, it is shown that the fine scale geometrical features can be captured; since FBM does not require re-meshing of fluid domain, no mapping of solutions from one time step to next, it is computationally very efficient; and the flow is accurately simulated.

The FBM is shown to be a powerful computational tool to be employed while working with complex arbitrary and/or moving geometries. This computational tool and the population balance implementation should be combined so that industrial or academic problems involving dispersed flows in complex geometries can be efficiently and accurately solved. This attempt requires efficient parallelization of the implementation of population balance model and FBM, which is our possible future work.

References

- [1] E. Bayraktar, O. Mierka, F. Platte, D. Kuzmin and S. Turek, *Numerical aspects and implementation of population balance equations coupled with turbulent fluid dynamics*, Computers & Chemical Engineering, Volume 35-11, 2011, 2204–2217. doi:doi:10.1016/j.compchemeng.2011.04.001
- [2] R. Münster, O. Mierka and S. Turek, *Finite Element Fictitious Boundary Methods (FEM-FBM) for 3D particulate flow*, International Journal for Numerical Methods in Fluids, 66: n/a. doi: 10.1002/flid.2558
- [3] Millies M. and Mewes D., *Interfacial area density in bubbly flow*, Chemical Engineering and Processing, **38**, 1999, pp.307-319.
- [4] Kuzmin D. and Turek S., *Numerical simulation of turbulent bubbly flows*, In: Proceedings of the Third International Symposium on Two-Phase Flow Modeling and Experimentation, Pisa, Italy, 2004.
- [5] McGraw R., *Description of aerosol dynamics by the quadrature method of moments*, Aerosol Science and Technology, **27**, 1997, pp.255-265.
- [6] McGraw R. and Wright D. L., *Chemically resolved aerosol dynamics for internal mixtures by the quadrature method of moments*, Journal of Aerosol Science, **34**, 2003, pp.189-209.
- [7] Fan R., Marchisio D. L. and Fox R. O., *Application of the direct quadrature method of moments to polydisperse gas-solid fluidized beds*, Journal of Aerosol Science, **139**, 2004, pp.7-20.
- [8] Bove S., *Computational fluid dynamics of gas-liquid flows including bubble population balances*, PhD Thesis, Aalborg University, Denmark, 2005.

- [9] Kumar S. and Ramkrishna D., *On the solution of population balance equations by discretization - I. A fixed pivot technique*, Chemical Engineering Science, **51-8**, 1996, pp.1311-1332.
- [10] Kumar S. and Ramkrishna D., *On the solution of population balance equations by discretization - II. A moving pivot technique*, Chemical Engineering Science, **51-8**, 1996, pp.1333-1342.
- [11] Chen P., Sanyal J., Duduković M. P., *Numerical simulation of bubble column flows: effect of different breakup and coalescence closures*, Chemical Engineering Science, **60**, 2005, pp.1085-1101.
- [12] Jakobsen H. A., Lindborg H., and Dorao C. A., *Modeling of bubble column reactors: progress and limitations*, Industrial Engineering and Chemical Research, **44**, 2005, pp.5107-5151.
- [13] Luo H. and Svendsen H. F., *Theoretical model for drop and bubble breakup in turbulent dispersions*, AIChE Journal, **42**, 1996, pp.1225-1233.
- [14] Coualoglou C. A. and Tavlarides L. L., *Drop size distributions and coalescence frequencies of liquid-liquid dispersions in flow vessels*, AIChE Journal, **22-2**, 1976, pp.289-297.
- [15] Tsouris C. and Tavlarides L. L., *Breakage and coalescence models for drops in turbulent dispersions*, AIChE Journal, **40**, 1994, pp.395-406.
- [16] Prince M. J. and Blanch H. W., *Bubble coalescence and break-up in air-sparged bubble columns*, AIChE Journal, **36**, 1990, pp.1485-1499.
- [17] H. Luo, *Coalescence, break-up and liquid circulation in bubble column reactors*, PhD. Thesis, The Norwegian Institute of Technology, Norway, 1993.
- [18] Lehr F., Millies M. and Mewes D., *Bubble size distribution and flow fields in bubble columns*, AIChE Journal, **48-11**, 2002, pp.2426-2442.
- [19] Buwa V. V. and Ranade V. V., *Dynamics of gas-liquid flow in a rectangular bubble column: experiments and single/multi-group CFD simulations*, Chemical Engineering Science, **57**, 2002, pp.4715-4736.
- [20] Glowinski, R., Pan, T.W., Hesla, T.I. and Joseph, D.D., *A Distributed Lagrange Multiplier/Fictitious Domain Method for Particulate Flows*, Int. J. Multiphase Flow, **25**, 755 – 794 (1999)
- [21] Patankar, N.A., Singh, P., Joseph, D.D., Glowinski, R. and Pan, T.W., *A New Formulation of the Distributed Lagrange Multiplier/Fictitious Domain Method for Particulate Flows*, Int. J. Multiphase Flow, **26**, 1509 – 1524 (2000)
- [22] Wan, D. and Turek, S., *An efficient multigrid-FEM method for the simulation of solid-liquid two phase flows*, J. Comput. Appl. Math., 203, 2, 561 – 580, 2007.

- [23] Wan, D. and Turek, S., *Direct Numerical Simulation of Particulate Flow via Multigrid FEM Techniques and the Fictitious Boundary Method*, International Journal of Numerical Methods in Fluids, 51, 5, 531 – 566, 2006
- [24] Wan, D. and Turek, S., *Fictitious Boundary and Moving Mesh Methods for the Numerical Simulation of Rigid Particulate Flows*, J. Comput. Phys., 22, 28 – 56, 2006.
- [25] Kuzmin D., Mierka O. and Turek S., *On the implementation of the k-epsilon turbulence model in incompressible flow solvers based on a finite element discretization*, International Journal of Computing Science and Mathematics, 1-2/3/4, 2007, pp.193 – 206.
- [26] Kuzmin D. and Möller M., *Algebraic flux correction I. Scalar conservation laws*, In: D. Kuzmin, R. Löhner and S. Turek (eds.), *Flux-Corrected Transport: Principles, Algorithms, and Applications*, Springer, Germany, 2005, pp.155 – 206.
- [27] Ramkrishna D., *Population Balances: Theory and Applications to Particulate Systems Engineering*, Academic Press, USA, 2000.
- [28] John V., Angelov I., Öncül A.A. and Thévenin, *Techniques for reconstruction of a distribution from a finite number of its moments*, Chemical Engineering Science, **62**, 2890 – 2904, 2007.
- [29] Gordon G. Roy, *Error bounds in equilibrium statistical mechanics*. Journal of Mathematical Physics, **9**-5, 655 – 663, 1967.
- [30] Turek, S., Wan, D.C. and Rivkind, L.S., *The Fictitious Boundary Method for the Implicit Treatment of Dirichlet Boundary Conditions with Applications to Incompressible Flow Simulations*, Challenges in Scientific Computing, Lecture Notes in Computational, Science and Engineering, Vol. **35**, Springer, 37 – 68 (2003).
- [31] Wan, D.C., Turek, S. and Rivkind, L.S., *An Efficient Multigrid FEM Solution Technique for Incompressible Flow with Moving Rigid Bodies*, Numerical Mathematics and Advanced Applications, ENUMATH 2003, Springer, 844 – 853 (2004).
- [32] Wan, D. and Turek, S., *Direct numerical simulation of particulate flow via multigrid FEM techniques and the fictitious boundary method*, International Journal for Numerical Methods in Fluids, 51, 5, 531–566, Published online 2005 in Wiley InterScience (www.interscience.wiley.com). doi: L 10.1002/fld.1129, 2006.
- [33] Miemczyk, M., *Hexaeder-Gittergenerierung durch Kombination von Gitterdeformations-, Randadaption- und Fictitious-Boundary-Techniken zur Strömungssimulation um komplexe dreidimensionale Objekte*, Diploma Thesis, TU Dortmund, 2007
- [34] Münster, R.: *Effiziente dynamische Suchdatenstrukturen zur Distanzberechnung in numerischen Strömungssimulationen*, Diploma Thesis, TU Dortmund, 2007